EUROPEAN ORGANIZATION FOR NUCLEAR RESEARCH

CERN-EP/85-75
14 May 1985

ANTIPROTONIC ATOMS AT LEAR: ACHIEVEMENTS AND PERSPECTIVES

H. Poth[1], P. Blüm[1], G. Büche[1], S. Carius[2], S. Charalambus[3], M. Chardalas[3], S. Dedoussis[3], C. Findeisen[4], A.D. Hancock[1], J. Hauth[1], H. Koch[1], T. Köhler[1], A. Kreissl[1], A. Nilsson[2], U. Raich[1], D. Rohmann[1], M. Suffert[5], L. Tauscher[4], A. Wolf[6], T. v. Egidy[7], F. Hartmann[7], W. Kanert[7], G. Schmidt[7] and J.J. Reidy[8]

Abstract: The outcome of the experimental study of the X- and gamma-ray spectra from antiprotonic atoms of Experiment PS176 is presented. First tentative results on the measurement of strong interaction effects in light $\bar{p}$ atoms are given. Isotope effects caused by strong interaction have been observed. From these data, information about the real to imaginary part of the $\bar{p}n$ forward scattering amplitude at zero energy was derived. An attempt was made to determine L–S dependence in the $\bar{N}N$ force.

Gamma spectra from nuclear fragments left over after $\bar{p}$ absorption were measured, and information about the frequency of $\bar{p}p$ to $\bar{p}n$ annihilation and single-nucleon removal was obtained.

For the first time the spectra of neutrons emitted from residual nuclei were also observed.

The fine-structure splitting of atomic levels was measured with high precision in order to determine the magnetic moment of the antiproton with greater accuracy.

The high-energy gamma spectra associated with $\bar{p}$ annihilation was measured in order to search for $\bar{p}$-nuclear and $\bar{p}$-nucleon states.

Moreover, a wealth of information on the antiprotonic atomic cascade was obtained.

Presented by H. Poth at the
Third LEAR Workshop on
Physics in the ACOL Era with Low-Energy Cooled Antiprotons,
Tignes, 19–26 January 1985

---

1) Kernforschungszentrum Karlsruhe, and Institut für Kernphysik, University of Karlsruhe, Fed. Rep. Germany.
2) Institute for Nuclear Research, Stockholm, Sweden.
3) Physics Department, Univ. of Thessaloniki, Greece.
4) Institute of Physics, Univ. of Basle, Switzerland.
5) Centre de Recherches Nucléaires, Strasbourg, France.
6) CERN Fellow.
7) Physics Department, Technical Univ., Munich, Fed. Rep. Germany.
8) Physics Department, Univ. of Mississippi, University, Miss., USA.

1. INTRODUCTION

At the first LEAR Workshop in Karlsruhe nearly exactly six years ago the study of the X-ray spectra from antiprotonic atoms was considered to be an important part of the LEAR experimental programme to investigate the $\bar{N}N$ interactions at zero energy [1]. The subject of exotic atoms has previously been reviewed by various authors [2], emphasizing the variety of information that can be obtained on hadron–nucleon interactions at rest. A compilation of pre-LEAR hadronic atom data can be found elsewhere [3].

Three years later, at the time of the Erice LEAR Workshop, most of the experiments were set up and eagerly awaiting the first beam time. At that meeting an outline of the potential physics of antiprotonic atoms, using the new antiproton facility, was given [4].

After 18 months of LEAR operation, this Workshop provides a good occasion for considering what has been achieved and what can be expected from future experiments using the technique of antiprotonic atoms. In this paper we present the outcome of experiment PS176 [5]. This was performed in close co-operation with PS186, and their results will be presented in the next paper [6].

2. EXPERIMENTAL GOALS

The experimental goal of PS176 was a survey measurement of strong interaction effects (shift ϵ and broadening Γ of atomic levels caused by $\bar{p}N$ interaction) in $\bar{p}$ atoms followed by a study of special aspects of the $\bar{p}N$ interaction. This study aimed, in particular, at the measurement of isotope effects due to the strong $\bar{N}N$ force, which previously proved to be a useful technique for disentangling $\bar{p}p$ from $\bar{p}n$ interactions [7], and at the eventual determination of the L–S dependence of the $\bar{N}N$ interaction. The latter can be deduced by measuring the shift and widths of resolved fine-structure levels [8]. Moreover, it was intended to combine these investigations with a spectroscopy of residual nuclei left over after $\bar{p}$ absorption in order to extract information about the modes of $\bar{p}$ annihilation in nuclear matter. It was also planned to search for possible narrow $\bar{p}$–nucleon or $\bar{p}$–nuclei states by measuring the high-energy gamma spectrum. The $\bar{p}$ absorption studies were to be complemented by the measurement of the spectrum of neutrons emitted from the nuclear debris in order to learn about the dissipation of the energy released in $\bar{p}$ annihilation at rest in nuclear matter.

The magnetic moment was determined with better precision, and abundant information on the antiproton atomic cascade could be obtained.

3. EXPERIMENTAL SET-UP

The experimental set-up is described in Ref. 4 and also in a forthcoming paper [9]. It consists essentially of a beam telescope to tag the incoming antiprotons, six high-resolution solid-state detectors, a large (10 in. × 12 in.) and a small (3 in. × 3 in.) NaI detectors, and a liquid scintillation neutron counter. The photon detection system spanned an energy range from 2 keV to 1 GeV. The targets (about 300 mg/cm^2) were mounted on a ladder to allow for a rapid exchange between beam spills. The data-acquisition system consisted of a fast front-end microprocessor with a large memory (2 Mbyte) for storing the time and energy of each detector event in two-dimensional histograms, and a background computer for monitoring count rates and controlling target and moderator positions. The system was designed to digest high event rates and to allow for a fast pre-analysis of the data. During past data-taking, almost no dead-time was encountered.

4. BEAM TIME, ANTIPROTON RATES, AND TARGETS

Experiment PS176 was performed at the m1 beam of LEAR with $\bar{p}$'s of 300 MeV/c and 200 MeV/c. The total running time between December 1983 and August 1984 was five days. Within this period, 63 spills (1 spill = 1 hour) of $\bar{p}$ beam were received. Of these, 7 spills were used to centre the beam on the target, to adjust the range of the $\bar{p}$'s so that they stop in the centre of the target, to optimize the detector settings, and to debug the data-acquisition system. The rest of the time was used for data production.

The number of $\bar{p}$'s accumulated was 5×10^9, corresponding to an average of 90 million $\bar{p}$'s per spill and an $\bar{p}$ rate of 25 kHz.

Table 1 gives detailed information on the measured targets and beam time.

Table 1

Summary of PS176 beam time

Nucleus studied	Target	Spills	Stopped antiprotons
^{16}O	H_2O	4	295×10^6
^{17}O	H_2O	11	816×10^6
^{18}O	H_2O	9	578×10^6
^{19}F	NaF	6	744×10^6
^{23}Na			
^{14}N	$Ba(NO_3)_2$	15	1373×10^6
^{138}Ba			
^{44}Ca	$CaCO_3$	1	206×10^6
^{70}Ge	Ge	3	213×10^6
^{208}Pb	Pb	7	526×10^6
10	8	56	4.8×10^9

5. RESULTS

5.1 Strong interaction effects in light nuclei

The energy shift ϵ (difference between measured and electromagnetic energy) and broadening Γ of the atomic 3d levels was measured in light nuclei between nitrogen and sodium. The width of the 4f level was also determined. The idea was to study the $\bar{p}$–nucleus interaction in this particular level over a range of nuclear targets in order to deduce a universal potential and to disentangle nuclear effects from elementary $\bar{p}$–nucleon interaction.

In these light nuclei the n → 3 transitions are the last observable X-ray lines of the atomic cascade prior to $\bar{p}$ annihilation. From the shift, width, and intensity of essentially the 4f → 3d transition, the strong interaction effects were determined. The X-ray spectrum of interest is shown in Fig. 1 for these light nuclei.

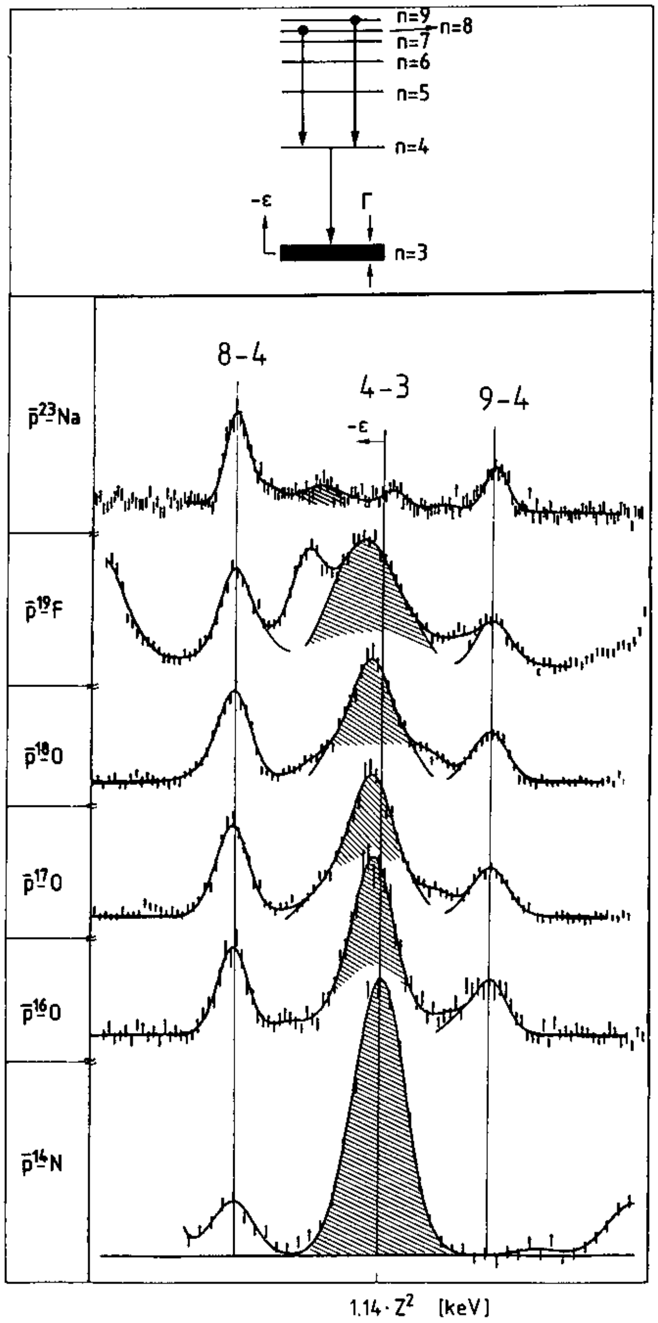

Fig. 1 Part of the X-ray spectrum of light antiprotonic atoms showing the unperturbed 8 → 4 and 9 → 4 lines and the 4 → 3 transition shifted in energy, broadened and attenuated. The ordinate is scaled for the different targets, so that the energy difference between the 8 → 4 and 9 → 4 is equal in all cases.

The 4 → 3 line is sandwiched between two transitions (8 → 4, 9 → 4) not affected by strong interaction. This fortunate situation provides an excellent means of calibration and allows for precision measurement.

The ordinate in Fig. 1 is scaled for the different targets in such a way that the positions of the unperturbed lines fall on top of each other. In this representation the strong interaction effects in the 4 → 3 line are clearly seen, increasing from nitrogen to sodium. In nitrogen the shift is invisible. The relative intensities of 8 → 4 and 9 → 4 may differ from target to target, depending on the atomic cascade.

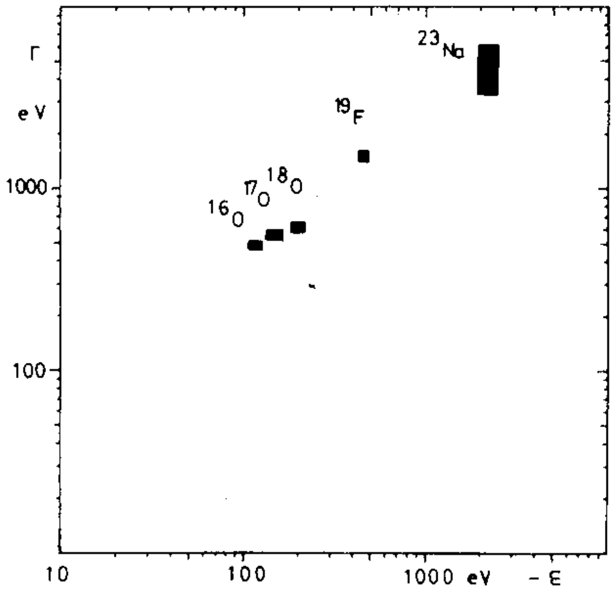

Fig. 2 Measured strong interaction width against shift in the 3d level of light antiprotonic atoms.

The measured strong interaction effects in the 3d level are displayed in Fig. 2 in an ε–Γ plot. The scaling is clearly visible.

A first attempt has been made to interpret these data in terms of an optical p̄-nucleus potential. So far, only the ^{16}O and ^{19}F data have been used to determine the real and imaginary parts of the effective p̄-nuclear scattering length. The tentative value is $A = (1.2 + i\,2.4)$ fm.

5.2 Isotope effects

Strong interaction effects were measured in all three stable oxygen isotopes in order to disentangle p̄p from p̄n interactions. For this purpose a comparative measurement was performed with an almost identical target arrangement. In Fig. 3 the X-ray spectra from the oxygen isotopes is shown. They are nearly identical, with the exception of the n → 3 transitions and the slight differences in X-ray energies due to the different reduced masses. The up-to-date evaluation of the strong isotope effect in the 3d level yields

$$^{18}\epsilon - {}^{16}\epsilon = -80\,(20)\ \mathrm{eV}, \qquad ^{17}\epsilon - {}^{16}\epsilon = -30\,(50)\ \mathrm{eV},$$
$$^{18}\Gamma - {}^{16}\Gamma = 160\,(40)\ \mathrm{eV}, \qquad ^{17}\Gamma - {}^{16}\Gamma = 90\,(50)\ \mathrm{eV}.$$

A preliminary interpretation of the isotope effect between ^{16}O and ^{18}O can be given in terms of a perturbation treatment [10], where the additional shift and broadening of the 3d level in ^{18}O with respect to ^{16}O is considered as a small perturbation. This additional potential can easily be related to the p̄n scattering length, considering the two valence neutrons in ^{18}O to be of low energy and quasi-free. Within this approach the difference in shift (width) is proportional to the real (imaginary) part of the p̄n scattering length. In order to get rid of common factors, one forms the ratio of shift to width:

$$2\,(^{18}\epsilon - {}^{16}\epsilon)/(^{18}\Gamma - {}^{16}\Gamma) = \mathrm{Re}\, a_{\bar{p}n}/\mathrm{Im}\, a_{\bar{p}n}\,.$$

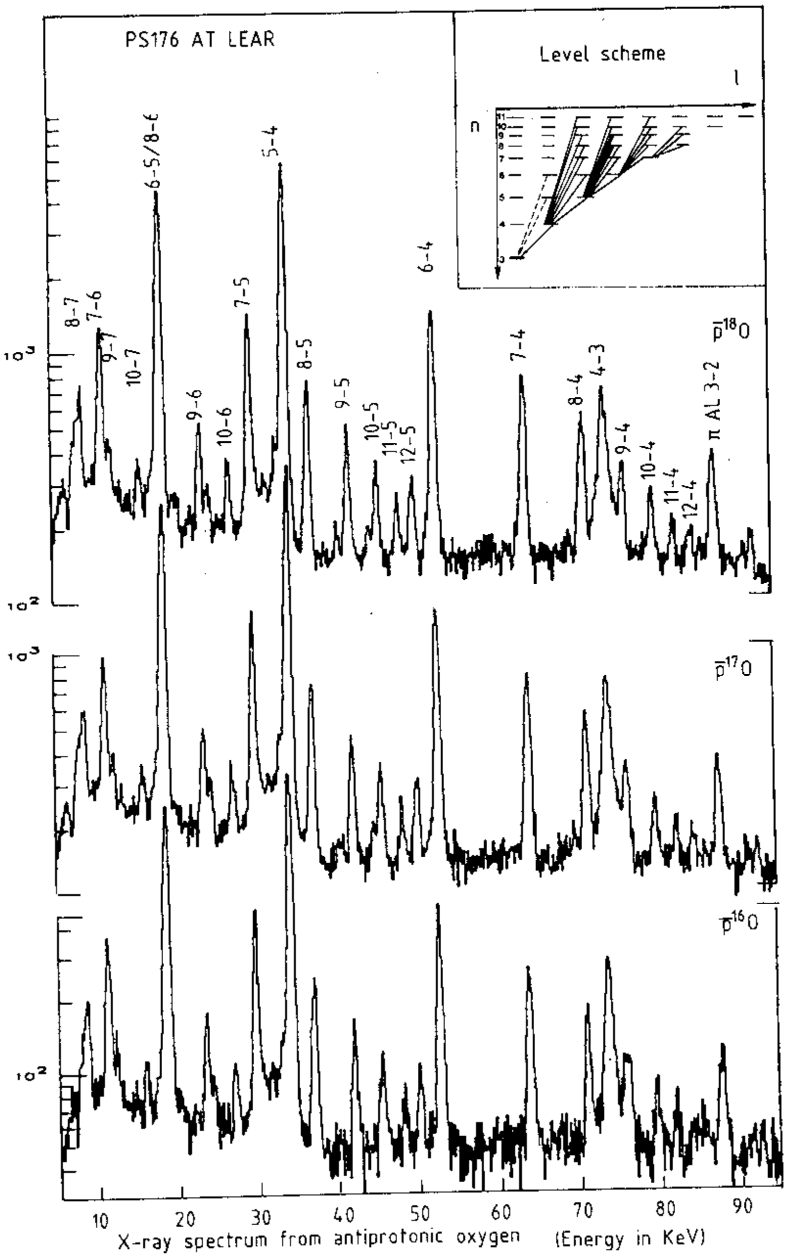

Fig. 3 X-ray spectra of $\bar{p}$-$^{16}O/^{17}O/^{18}O$.

This is the ratio of the real to imaginary part of the $\bar{p}n$ scattering amplitude ($\varrho_{\bar{p}n}$) at zero energy. From our $^{18}O/^{16}O$ data we deduce: $\varrho_{\bar{p}n} \approx -1$.

5.3 L–S dependence of the $\bar{N}N$ force

From the measurement of the strong interaction effects in resolved fine-structure levels of $\bar{p}$ atomic states, a possible L – S dependence of the $\bar{p}$-nucleus interaction can be deduced [8]. It would show up as a difference in shift and width in the two fine-structure levels (spin-angular momentum parallel and antiparallel, respectively). In order to reach a high level of sensitivity, one needs to find a spinless nucleus and atomic levels where the total strong interaction width is less than the fine-structure splitting but still large enough to be measurable with an accuracy of better than, say, 5%. According to our estimates the

$8 \rightarrow 7$ transition in ^{138}Ba would fulfil these conditions. We have measured the X-ray spectrum of ^{138}Ba and resolved the fine-structure components of the 7i level. The total shift (width) of this level is 350 (1800) eV. The purely electromagnetic fine-structure splitting is 2.1 keV. With the present sensitivity (about 45% for ϵ and 25% for Γ, limited merely by statistics) we do not observe an L–S effect. Obviously more statistics are needed.

5.4 Antiproton absorption

This aspect was studied in three different ways. Firstly, a spectroscopy of gammas emitted from excited residual nuclei left over after $\bar{p}$ absorption was performed; secondly, the spectrum of the emitted neutrons was measured; and thirdly, high-energy gammas in the range between a few tens of MeV and 1 GeV were detected. These data were recorded for almost all the investigated targets. For instance, for oxygen, we can already state observations of the following reactions:

$$\bar{p} + {}^{18}\mathrm{O} \rightarrow (\bar{p}n) + {}^{17}\mathrm{O}^* (\tfrac{1}{2}^+ \text{ or } \tfrac{1}{2}^-) \rightarrow \left\{\begin{array}{ll} {}^{17}\mathrm{O}^*(\tfrac{1}{2}^+) & + \ \gamma \ \ (871\ \mathrm{keV}) \\ {}^{17}\mathrm{O} & + \ \gamma\ (2184\ \mathrm{keV}) \end{array}\right\} + X$$

$$\bar{p} + {}^{18}\mathrm{O} \rightarrow (\bar{p}p) + {}^{17}\mathrm{N}^* (\tfrac{5}{2}^- \text{ or } \tfrac{1}{2}^+) \rightarrow \left\{\begin{array}{l} {}^{17}\mathrm{N} + \gamma\ (1907\ \mathrm{keV}) \\ {}^{17}\mathrm{N} + \gamma\ (1850\ \mathrm{keV}) \end{array}\right\} + X$$

$$\bar{p} + {}^{18}\mathrm{O} \rightarrow \begin{bmatrix} (\bar{p}n) + p \\ (\bar{p}p) + n \\ \bar{p}d \end{bmatrix} + {}^{16}\mathrm{N}^* (1^- \text{ or } 3^-) \rightarrow \left\{\begin{array}{ll} {}^{16}\mathrm{N}^*(0^-) & + \ \gamma\ (278\ \mathrm{keV}) \\ {}^{16}\mathrm{N} & + \ \gamma\ (297\ \mathrm{keV}) \end{array}\right\} + X + \text{nucleon}$$

$$\bar{p} + {}^{17}\mathrm{O} \rightarrow (\bar{p}p) + {}^{16}\mathrm{N}^* (3^-) \rightarrow {}^{16}\mathrm{N} + \gamma\ (297\ \mathrm{keV}) + X$$

$$\bar{p} + {}^{17}\mathrm{O} \rightarrow (\bar{p}p) + {}^{16}\mathrm{N}^* (1^-) \rightarrow \text{not observed}$$

(X means annihilation products)

The data are being evaluated. However, already at the present stage one can state that the $\bar{p}$ annihilation in light nuclei on a single nucleon with an intact residual nucleus left over in an excited state is unexpectedly frequent.

Neutrons emitted from residual nuclei after $\bar{p}$ absorption were measured in the energy range between 1 MeV and about 100 MeV with a liquid-scintillation counter. The spectra are similar for all targets. One can distinguish essentially three regions in the spectrum: evaporation neutrons corresponding to a temperature of about 7 MeV; faster neutrons with temperatures around 45 MeV; and a few very fast neutrons. The neutron multiplicities determined are of the order of 3 for oxygen and 7.3 for lead.

The high-energy gamma spectrum shows no obvious evidence for possible $\bar{p}$–nucleon or $\bar{p}$–nucleus bound states.

5.5 Magnetic moment measurement

The magnetic moment of the $\bar{p}$ was remeasured by extracting the electromagnetic fine-structure splitting in the $11 \rightarrow 10$ and the $10 \rightarrow 9$ transitions in $\bar{p}$–^{208}Pb. In Fig. 4 the relevant X-ray transitions are shown. One

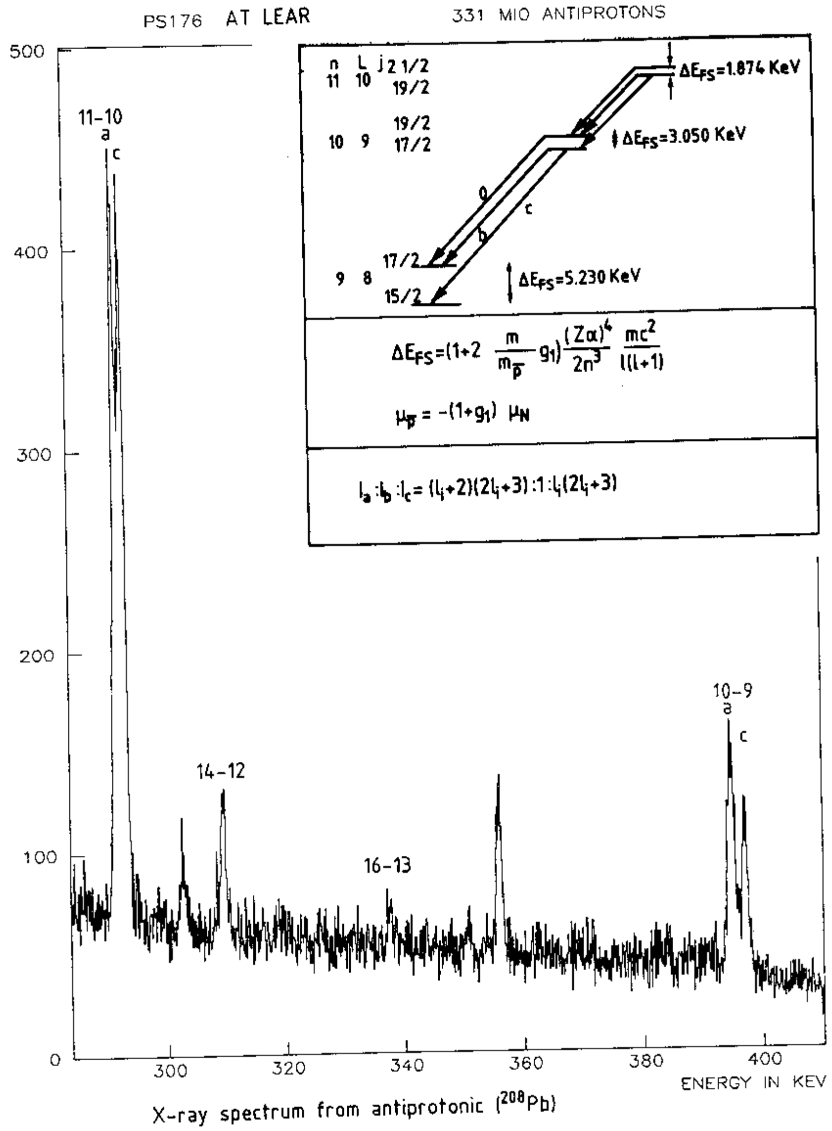

Fig. 4 Part of the p̄–Pb spectra showing the X-ray transition used to determine the magnetic moment of the antiproton.

clearly observes the two most intensive components resolved, which are separated by 2.1 (1.2) keV for the 10 → 9 (11 → 10) transitions. With the present statistics we will be able to determine the magnetic moment with a precision of the order of 3×10^{-3}, i.e. a factor of 2 better than the actual world average.

5.6 Precision energy measurement of antiprotonic X-rays

We performed a feasibility study to measure the energy of a particular X-ray transition with very high accuracy by using the critical absorber technique. This method makes use of the rapid change with energy of the photoabsorption cross-section in the region of an absorption edge. By comparing the intensity and line shape of an X-ray (whose energy falls on top of the absorption edge) which passed through the absorber foil, with the directly measured one, it is possible to determine its energy rather accurately.

After a careful scan of calculated p̄ X-ray energies and a comparison with absorption edge energies, we found a promising candidate in ^{70}Ge (9 → 8 transition) and the K_β edge of Hg. In our test measurement on

^{70}Ge we verified this energy degeneracy and observed a very clear effect. With this method we hope to arrive at an absolute energy determination with an error below 1 eV.

The purpose of this measurement is manifold. On the one hand it could serve as an energy standard for determining the $\bar{p}$ mass with high precision; on the other hand, other effects which could alter the $\bar{p}$ X-ray energies, such as nuclear and $\bar{p}$ polarizability or long-range contributions of the $\bar{N}N$ force, could be traced out.

6. DISCUSSION OF RESULTS

Hopefully this paper shows that the data from $\bar{p}$ atoms accumulated within a few days of LEAR beam time provide a large amount of new information.

Pre-LEAR data on strong interaction effects in $\bar{p}$ atoms had been analysed by many theoretical groups [11-17]. Their predictions for shifts and widths are given in Table 2 together with our new tentative data.

It should be noted that the strong interaction effects have been measured to an unprecedented precision and it is evident that these new data will provide better constraints on the $\bar{N}N$ potential. It is intended to analyse $\bar{p}$ atomic data and $\bar{p}$–nucleus scattering data together in the frame of an optical potential. As a first

Table 2

Strong interaction shifts (upper line) and widths (lower line) of $\bar{p}$ atomic levels.
Values are given in eV; the statistical errors are in brackets*).
(In the case of several theoretical values given by the same authors for a certain nucleus, those which come closest to our experimental results are taken)

Nucleus	Level (transition)	Electromagnetic transition energies	PS176	Ref. 11	Ref. 12	Ref. 13	Ref. 14	Ref. 15	Ref. 16	Ref. 17
^{14}N	3d	55828		−51	−171			−53	−31	
	(4 → 3)		100 (50)	141	175	163		167	148	
^{16}O	3d	73570	−120 (20)	−148	−116		−90	−161	−134	−125
	(4 → 3)		480 (30)	67	547	532	554	444	578	652
^{17}O	3d	73828	−150 (50)							−155
	(4 → 3)		550 (50)							858
^{18}O	3d	74059	−200 (20)				−158	−195		−181
	(4 → 3)		620 (30)			646	688	503		750
^{19}F	3d	94029	−470 (20)							
	(4 → 3)		1490 (50)							
^{23}Na	3d	141799	−2200 (260)							
	(4 → 3)		4700 (1400)							
^{138}Ba	7i	375414	−350 (150)							
	(8 → 7)		1800 (450)							

*) The values given have to be considered preliminary as only part of the data are evaluated.

step in this direction, we find from the analysis of our oxygen data a similar ratio for the real to imaginary part of the optical potential parameters as seen from the p̄-O scattering data [18], namely about 0.5.

The $\varrho_{\bar{p}n}$ value at zero energy, which we determined from our isotope measurements, has negative sign and an absolute value close to unity. Compared with measurements of $\varrho_{\bar{p}p}$ determined from the interference of Coulomb and strong interaction observed in elastic p̄p scattering [19, 20], and with dispersion relation analysis [21], this indicates an unusual behaviour of the N̄N scattering amplitude close to threshold. The negative sign is also supported by the observed negative shift of the 1s level in antiprotonic hydrogen [22, 23].

7. PERSPECTIVES

Within the little beam time available for p̄-atom studies at LEAR, a lot of new information could be extracted. However, the field is far from being fully exploited and most of the perspectives outlined at Erice [4] have not yet been tackled. Still more precise data on strong interaction effects over a wider range of nuclei are needed. In particular those nuclei have to be examined where strong interaction effects fall into the detection window (i.e. $300\ \mathrm{eV} \leqslant \Gamma \leqslant 5\ \mathrm{keV}$, $-\epsilon \geqslant 50\ \mathrm{eV}$) and where the intensity of the last observable transition is still large enough to allow for the accumulation of sufficient statistics.

Specific aspects have to be studied in more detail. That is primarily the L–S dependence and the isotope effect. In both cases the precision can be improved. Increasing precision will eventually allow also the separation of hyperfine states and thus provide a means of studying spin–spin effects. These aspects are of extreme relevance for the investigation of the N̄N interaction as the p̄-atom method offers the possibility to filter out specific terms of the N̄N potential.

As it concerns the more detailed investigation of p̄-absorption, coincidence experiments are definitely required. Let us consider, for instance, the observed reactions presented under subsection 5.4. There an X-γ-ray or a γ-ray–neutron coincidence would reveal valuable information on the dynamics of the p̄ absorption. For example the identification of a ^{16}N residual nucleus after p̄ annihilation in ^{18}O in coincidence with the spectroscopy of the single neutron would allow the extension of the p̄p interaction study below threshold. Second-generation experiments certainly could satisfy this requirement, applying highly developed detectors (e.g. a crystal spectrometer and multiple solid-state detector arrays) and specialized triggers (X-ray and gamma-ray coincidences or triggers on particular absorption products).

We also want to point out that the p̄-atom method provides an interesting possibility for investigating other particular modes of p̄ annihilation [24]: namely, the p̄ annihilation on two nucleons, opening up the channel for strange hyperon production (Σ, Ξ). Recently, it was conjectured that this process could amount to a few permille in p̄ annihilation in nuclear matter [25]. This could be studied by stopping in the target the negative hyperon, which has low energy, and forming a hyperonic atom which identifies itself through its X-ray transitions. It should be possible to achieve a sensitivity of 10^{-3} for measuring the branching ratio of p̄ annihilation into negative hyperons (Σ^-, Ξ^-), with only 10^9 stopped p̄'s.

REFERENCES

1) E. Klempt, Antiprotonic atoms, Proc. Joint CERN-KfK Workshop on Physics with Cooled Low Energetic Antiprotons, ed. H. Poth (KfK-Bericht 2647, Karlsruhe, 1979), p. 161.

2) C.S. Wu and J. Willets, Ann. Rev. Nucl. Sci. **19**, 527 (1969).
G. Backenstoss, Ann. Rev. Nucl. Sci. **20**, 497 (1970).
R. Seki and C.E. Wiegand, Ann. Rev. Nucl. Sci. **25**, 241 (1975).
H. Koch, Muonic and hadronic atoms at intermediate energies, ed. J.B. Warren (Plenum Press, Inc., New York, 1976), p. 87.
C. Batty, Nucl. Phys. **A372**, 433 (1981).

3) H. Poth, Compilation of data from hadronic atoms (Physics Data Report 14-1, Fachinformationszentrum, Karlsruhe, 1979).

4) H. Poth, Physics of antiprotonic atoms, Proc. 2nd LEAR Workshop on Physics with Low-Energy Cooled Antiprotons, Erice , 1982, eds. U. Gastaldi and R. Klapisch (Plenum Press, Inc., New York, 1984), p. 567.

5) PS176 Collaboration (Spokesman H. Poth), Proposal CERN/PSCC/80-103 (1980).

6) W. Kanert et al., this Workshop.

7) H. Poth et al., Nucl. Phys. **A294**, 435 (1978).

8) H. Poth, Strong interaction effects in resolved fine-structure levels of antiprotonic atoms, Contribution to the CERN Intermediate-Energy Physics Workshop, CERN, Geneva, 1977 (unpublished).

9) T. Köhler et al., Precision measurement of strong interaction isotope effects in ^{16}O, ^{17}O, and ^{18}O, to be submitted to Physics Letters B.

10) H. Poth, KfK-Bericht 2613, Karlsruhe (1976) and The real to imaginary part of the $\bar{N}N$ forward scattering amplitude at zero energy from $\bar{p}$-atoms, in preparation.

11) J.F. Haak, A. Lande and F. Iachello, Phys. Lett. **66B**, 16 (1977).

12) H. Nishimura and T. Fujita, Phys. Lett. **60B**, 413 (1976).

13) W. Kaufmann and H. Pilkuhn, Phys. Lett. **62B**, 165 (1976).

14) A.M. Green and S. Wycech, Nucl. Phys. **A377**, 441 (1982).
A.M. Green, W. Stepien-Rudzka and S. Wycech, Nucl. Phys. **A399**, 307 (1983).

15) T. Suzuki and H. Narumi, Nucl. Phys. **A426**, 413 (1984).

16) A. Deloff and J. Law, Phys. Rev. **C10**, 2657 (1974).

17) S. Dumbrajs et al., this Workshop.

18) D. Garetta et al., Phys. Lett. **135B**, 266 (1984) and **139B**, 464 (1984).

19) L. Linsen et al., this Workshop.

20) T.A. Shibata et al., this Workshop.

21) W. Grein, Nucl. Phys. **B131**, 255 (1977).

22) C. Batty et al., this Workshop.

23) R. Landua et al., this Workshop and S. Ahmad et al., CERN Preprint CERN EP/84-85 (1984).

24) H. Poth, Multinucleon $\bar{p}$ absorption and hyperonic atom formation, in preparation.

25) J. Cugnon and J. Vandermeulen, Phys. Lett. **146B**, 16 (1984).